Journal of the Australian Ceramic Society (2023) 59:245–257
https://doi.org/10.1007/s41779-022-00830-2

RESEARCH

Improving properties of biodegradable chitosan/PVA composite polymers via novel designed ZnO particles

Yeliz Köse[1,2] · **Ender Suvacı**[1,3] · **Burcu Atlı**[3]

Received: 26 September 2022 / Revised: 19 December 2022 / Accepted: 26 December 2022 / Published online: 11 January 2023

Abstract

Biodegradable polymers exhibit great potential to be a critical part of the global sustainability solution; however, their application areas are limited due to their inadequate properties for some applications. Although nano metal oxide powders are often used to improve the properties, they exhibit toxicity, phytotoxicity and uncontrolled agglomeration. Recently, designed, micron size, hexagonal platelet particles, which constitute fine primary particles (MicNo®), have been manufactured to exploit advantages of both micron and nano size, while abating the adverse effects of nanoparticles. Accordingly, the research goal of this study was to appraise effects of MicNo® ZnO and Ag-doped MicNo® ZnO particles on structure development and hence properties of chitosan/PVA films. The results show that MicNo® particles improve UV-resistance, mechanical and antibacterial properties of the films much more effectively with respect to nanoparticles due to their novel morphology and demonstrate great potential as new generation additive systems for biodegradable polymers to extend their application areas.

Keywords Chitosan · Polyvinyl alcohol · Zinc oxide · Ag doping · Antibacterial activity · UV-blocking

Introduction

"Transforming Our World: The 2030 Agenda For Sustainable Development" document is a universal call to action that includes 17 goals aimed to be achieved by the member states of the United Nations by the end of 2030. The 12th Objective of this document is *Responsible Production and Consumption*. The content of Article 4 of the 12th Target is stating that by 2030, it is aimed to significantly reduce the emissions of chemicals and all wastes to nature in order to minimize their negative effects on human health and the environment. Accordingly, this declaration and many other actions have increased the search activities on environmentally benign and sustainable materials development. Biodegradable polymers have already started to take the place of conventional polymers as a result of the increase in environmental awareness created by many actions including the universal and increasing the demand for environmentally friendly materials.

Although agropolymers have low decomposition temperature and mechanical strength, they are one of the most preferred biodegradable materials due to their low cost and non-toxicity and constitute 40% of the polymer industry [1]. Studies on chitosan, which is one of the agro polymers, are increasing day by day because of its widespread usability and abundancy in nature and it does not show toxic effects. Furthermore, it is biodegradable, biocompatible and inhibits microorganisms [2]. The properties of chitosan depend on the degree of deacetylation, molecular weight, source of chitosan and preparation technique. Chitosan with low molecular weight and high degree of deacetylation exhibits high antibacterial and hemostatic properties [3]. It is used in medical applications as wound healing due to its ability to inhibit fibroplasia and support tissue growth [4], in photography due to its optical characteristics and film forming ability [5], in cosmetics due to its easy dissolution in organic acids and fungicidal-fungistatic properties [6], and in packaging applications due to its optical clarity, mechanical stability and gas permeability properties [7]. On the other

✉ Yeliz Köse
yelisskose@gmail.com

Ender Suvacı
esuvaci@eskisehir.edu.tr

[1] Department of Materials Science and Engineering, Eskisehir Technical University, TR26480 Eskisehir, Turkey

[2] Department of Metallurgy and Materials Engineering, Bilecik Şeyh Edebali University, TR11210 Bilecik, Turkey

[3] R&D Laboratories, Entekno Corp, TR26004 Eskisehir, Turkey

hand, there are some disadvantages of pure chitosan such as poor mechanical properties, dissolution only in acidic media, and loss of its antibacterial activity at pH > 6.5 [8]. The most effective method to overcome these disadvantages is blending with other polymers such as gelatin [9], polylactic acid (PLA) [10], polyvinyl alcohol (PVA) [11] etc. Polyvinyl alcohol (PVA) is a widely used polymer with chitosan due to its advantages such as water solubility, hydrophilic structure, biocompatibility, chemical resistance, natural adhesiveness and easy modification of hydroxyl groups [12]. In addition, by blending chitosan with PVA, both antimicrobial activity and UV absorption can be achieved [13].

Low molecular weight plasticizers reduce the deformation stress, stiffness, density, viscosity, and electrostatic charge of a polymer, while increasing chain flexibility, resistance, and dielectric constant [14]. Glycerol has been widely used as a plasticizer for films of the chitosan. It reduces intermolecular interaction, increases free volume, and facilitates molecular movements [15]. Thus, glycerol can be effectively utilized as a polymeric additive to improve flexibility and chemical permeability [16].

Unfortunately, the use of biodegradable polymers is limited because of several reasons such as inadequate performance (brittleness, poor barrier properties) for specific applications, processing limitations (low thermal strength temperatures) and cost [17]. The incorporation of nanoparticles (Ag, Cu, TiO_2, ZnO) to these polymers has been used to overcome these drawbacks. However, these nanoparticles have advantages or disadvantages depending on their particle size, chemical composition, crystallinity and shape [18].

Recently, antimicrobial activity has been improved by preparing different metal chitosan complexes such as Ag^{+} [19] and Cu^{+2} [20]. Antimicrobial activities of Ag nanoparticles have been proven to be higher than other metal nanoparticles according to the following order Ag > Cu > Au > Zn > Fe [21]. In addition, bimetallic nanoparticles such as Ag–Cu are more preffered than single metalic nanoparticles as they further improve the optical and antimicrobial properties of food packaging materials [22]. Tan et al. [23] showed that although Ag and Cu nanoparticles once accumulated in the body are released through hair, urine and feces; the difficulty of its complete removal from animal and human tissues has been proven. Although long-term toxicity to human and animal cells is unclear, caution is recommended when applying Ag and Cu nanoparticles to different parts of the body.

TiO_2 is widely used as a filler in biodegredable polymers due to its low cost, biocompatibility, thermal stability, physicochemical, mechanical and photocatalytic properties [24]. However, Ghosh et al. [25] determined the toxic effect of commercial TiO_2 nanoparticles on human and animal cells. The cytotoxic effects of TiO_2 nanoparticles against human lymphocyte cells appeared to be dependent on the stability of the membrane, mitochondria, metabolic activity, and lysosomal membrane. Therefore, caution is recommended when applying TiO_2 nanoparticles to different parts of the body.

The use of ZnO is increasing as it improves the external durability, antibacterial and physico-mechanical properties of chitosan-based biodegradable films [26]. ZnO nanoparticles exhibit strong antibacterial properties against different bacterial species, as reported in the literature. The role of particle size of ZnO nanoparticles on their antibacterial behavior is not clear. In the studies of Jones et al. [27], it was observed that the toxicity increased with the decrease of ZnO particle size, while in the studies of Franklin et al. [28] it was found that the particle size had no effect on toxicity. The use of ZnO nanoparticles in cosmetic products is considered advantageous due to their high antibacterial activity and UV absorption capacity [29]. Doping ZnO nanoparticles with transition metals because of ion release has been used for increasing antibacterial activity performance of ZnO besides its broad spectrum UV protection [30–32]. However, such nanoparticles can introduce some difficulties. For example, nanoparticle additives increase transparency but cause uncontrolled agglomeration due to the high surface area/volume ratio and hence high surface energy. Then such agglomerates reduce the local mechanical strength [33]. Accordingly, there is a need for alternative additive forms which will be safe and biocompatible as well as transparent and provide both UV-resistance and antibacterial effect. Recently, a novel particle technology, called MicNo® was developed by Suvacı and his co-workers [34]. MicNo® particles are designed micron size hexagonal platelets which are composed of primary fine particles. They only exhibit advantages of micron and nano size while mitigating their disadvantages such as uncontrolled agglomeration. For example, they exhibit superior surface coverage (up to 70% more) with respect to spherical particles while they are transparent.

In previous studies, MicNo® particles' performance as antistatic coating materials [35]; their biocompatibility and their in vitro cytotoxicity, genotoxicity, phototoxicity behaviors on human epidermal keratinocyte (HaCaT) cells [36]; their antimicrobial activity against 11 different microorganisms [34]; their usability as electrode materials in Li-ion batteries [37] were investigated. The performance of MicNo® forms in biodegradable polymers has not been previously studied. Consequently, the research objective of this study was to appraise how MicNo® forms affect the mechanical, optical, antibacterial and UV-blocking properties of the chitosan/PVA biodegradable films. Therefore, in this study, MicNo® ZnO and MicNo® Ag doped–ZnO inorganic powders were added to CS/PVA composite films to achieve this objective.

Table 1 Used powder systems in composite films and their names

Sample no	Sample	Sample name
1	0 (wt.%) ZnO doped chitosan/PVA Film	ZnO-0
2	2.5 (wt.%) nano-ZnO doped chitosan/PVA Film	ZnO-N
3	2.5 (wt.%) MicNo® -ZnO doped chitosan/PVA Film	ZnO-M
4	2.5 (wt.%) MicNo® -Ag ZnO doped chitosan/PVA Film	ZnO-AM

Experimental procedure

Materials

Chitosan (CS) with low molecular weight and degree of deacetylation of 75% by CDH was used. In addition, PVA with average molecular weight of 135,000–205,000, glacial acetic acid and glycerol with molar weight 92.09 g/mol by Sigma-Aldrich Co. LLC were utilized. Undoped and Ag-doped MicNo® ZnO (12 wt.%) inorganic powders with 2–10 µm sized hexagonal platelet aggregates of 30–100 nm size particles were supplied by Entekno Materials Inc. Nano ZnO inorganic powder with < 100 nm individual size particles by Sigma-Aldrich Co. LLC. was used as a reference material for bench-marking. *Escherichia coli* (ATCC 8739) and *Staphylococcus aureus* (ATCC 6538) strains were preferred to investigate the antibacterial activity of the film systems as representative microorganisms of gram-negative and gram-positive bacteria, respectively.

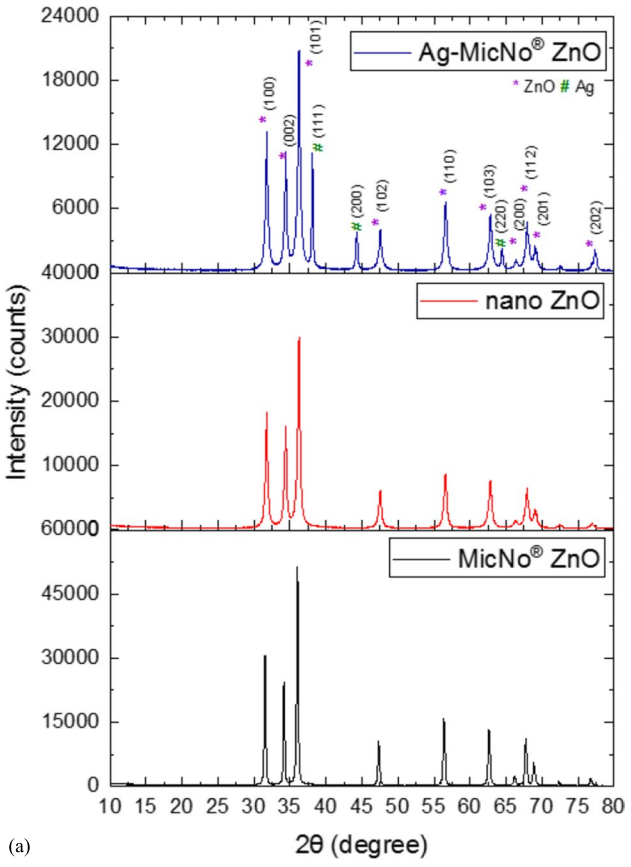

(a)

Fig. 1 (**a**) XRD patterns of the studied powders and (**b**) SEM micrographs of i) undoped nano ZnO, (ii) undoped MicNo® ZnO, (iii) Ag-doped MicNo® ZnO

Preparation of CS/PVA/ZnO composites film

CS (3 g) was first dissolved in 100 mL of 3% aqueous acetic acid solution and PVA (15 g) was dissolved in 100 mL water at 80 °C. Both of the clear solutions were kept overnight while they were being stirred. After that, the PVA solution (30 mL) was added to the CS solution (20 mL) while it was being magnetically stirred to get clear solution. Then, nano ZnO or MicNo® ZnO or Ag-doped MicNo® ZnO (1500 mg) and glycerol (10 mL) were added into the chitosan/PVA solution which was at 80 °C and stirred by keeping overnight. The obtained gel-like viscous solution was poured onto a plastic substrate and the films with a thickness of 300 µm were prepared by tape casting technique and dried in air at room temperature for 24 h. In Table 1, the designations of the samples that were studied in this project, are shown. Prior to tests, the films were cut into specific size and their width and length.

Materials characterization

X-ray diffraction (XRD) analyses were performed by D2 Phaser (Bruker, Cu $K\alpha = 1.54$ Å) for phase determination. The Fourier transformed infrared (FTIR) spectra were collected by IRTracer-100 (Shimadzu, the wavelength range of 4000–400 cm^{-1}). The size and morphology of the particles were examined with scanning electron microscopy (SEM EVO 50 LP, Zeiss, operating at 10 kV). The optical measurements were conducted by UV–VIS-NIR spectrophotometer (UV-3600 Plus UV–VIS-NIR, Shimadzu) in a wavelength range of 260–750 nm. The mechanical analyses were performed in a universal testing machine (INSTRON 5581) with 5 samples in each case with a dimension of 100 × 20 mm. Antibacterial activities of films were tested with two different methods (inhibition zone assay and ISO 22196:2011 standart) [38]. Antibacterial activity was calculated according to the ISO

(b) i.

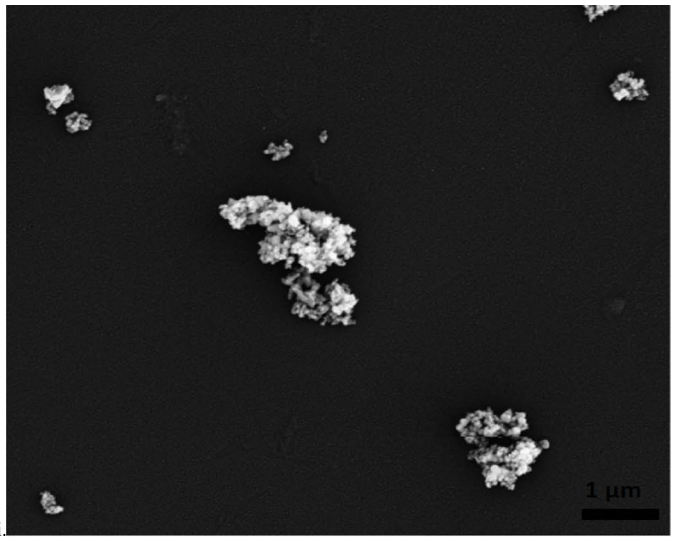

ii.

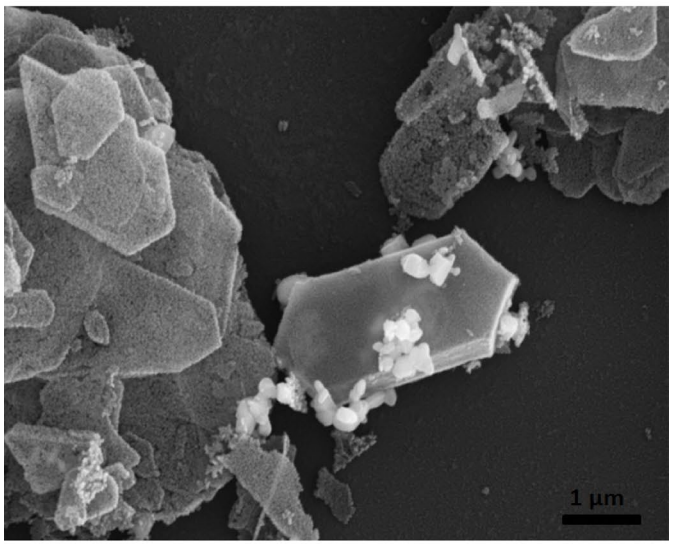

iii.

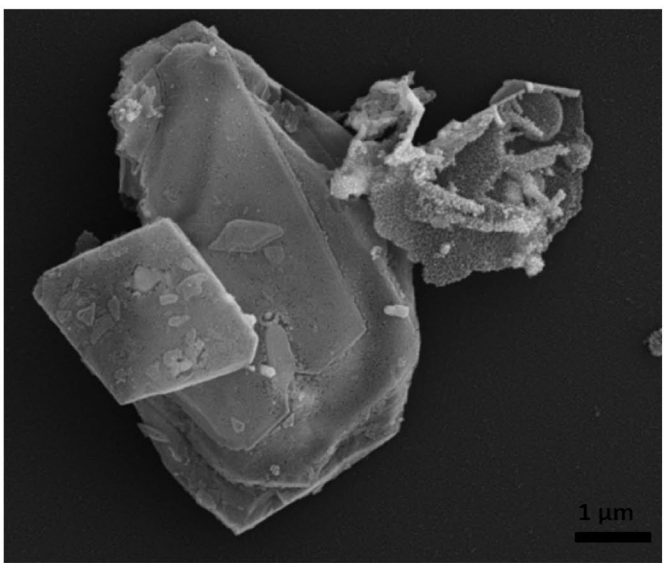

Fig. 1 (continued)

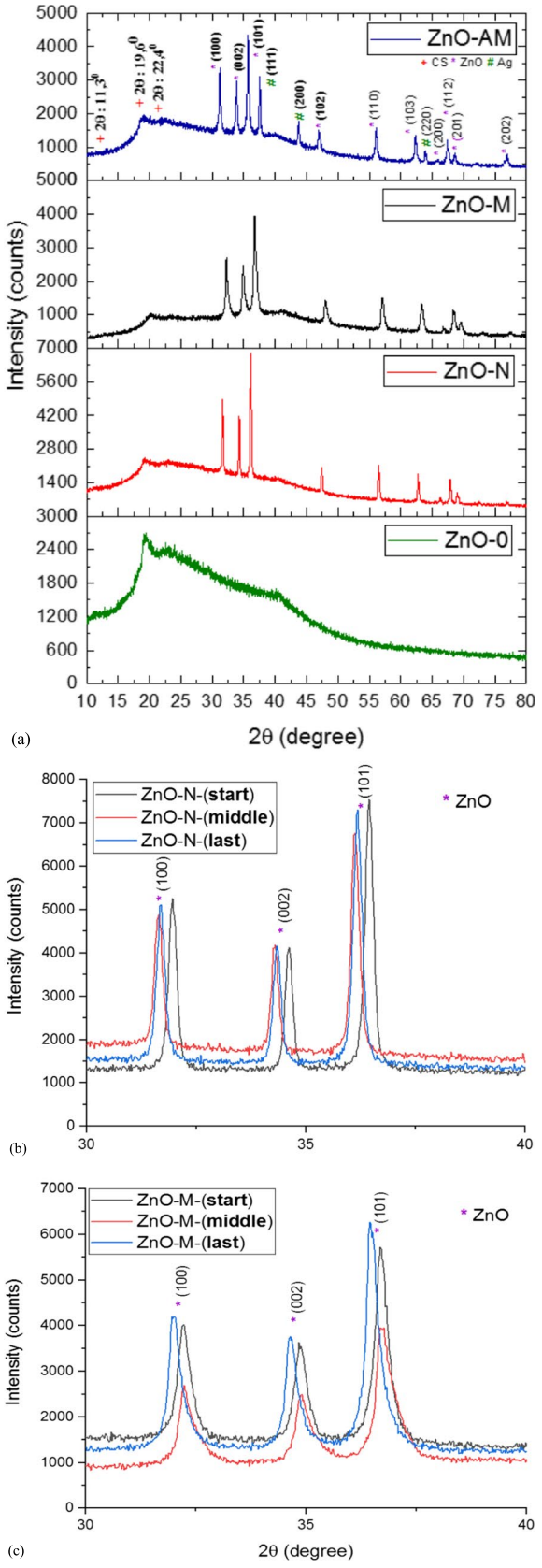

Fig. 2 (**a**) XRD patterns of the studied films and XRD patterns comparison of the start-middle-end parts of (**b**) ZnO-N (**c**) ZnO-M film

22196:2011 standard, the antibacterial activity value of a surface should be $R \geq 2$.

Results and Discussion

Characterization of the powders

Figure 1a shows the XRD patterns of the powder systems used in this study. According to the XRD patterns both nano and MicNo® ZnO powders exhibit single phase ZnO with hexagonal wurtize type crystal structure (JCPDS card no: 36–1451) [39]. This means that both nano and MicNo® ZnO powders are chemically and cyrstallagrophically very similar materials. XRD pattern of Ag-doped MicNo® ZnO particles also demonstrates presence of metallic Ag peaks besides shifted ZnO peaks which indicates enterance of Ag^{+} ions into the ZnO lattice [40]. It was observed that the characteristic peak of the (101) plane shifted to lower 2θ values (i.e. higher interplanar spacing) in the MicNo® Ag-ZnO doped. Since lattice expansion is anticipated due to the ionic size difference between the Ag^{+} (1.26 Å) and Zn^{+2} (0.74 Å) ions, the characteristic peak is expected to shift to lower 2θ values [41]. These results are in agreement with Demirel R. et al. [34] and Şahin (Şahin İ. M.Sc.Thesis) where they reported that Ag-metal particles exist in MicNo® ZnO platelets as an anchored part of the MicNo®-form instead of isolated particles. Figure 1b (i) shows SEM micrograph of the nano ZnO particles which have spherical-coaxial shape. Figures 1b (ii) and (iii) exhibit SEM micrographs of the MicNo® ZnO and Ag-doped MicNo® ZnO particles, respectively. It can be seen by SEM micrographs that the MicNo® particles are composed of primary fine particles. The micrographs show that all particles have similar hexagonal platelet morphology which are 2–10 µm long and 30–100 nm thick. Due to the transparency of the platelets, even if they overlap, they can be distinguished by SEM images [34]. These results show that while nano and MicNo® ZnO particles are chemically the same, they are different in terms of their morphologies.

Effects of MicNo® particles on structure development of the chitosan/PVA Films

Figure 2a shows the XRD patterns of the films evaluated in this study. The XRD patterns of the film show that the chitosan/PVA films exhibit same characteristic peaks at 11.3°, 19.6° and 22.4° 2θ values [42]. XRD patterns of the doped films demonstrate peaks which are combination of both the polymeric part and the additives. Figure 2b and c shows the XRD patterns comparison of the start-middle-end parts of ZnO-N film and ZnO-M films, respectively. The intensities of characteristic peaks of ZnO are very close to each other. It should be noted

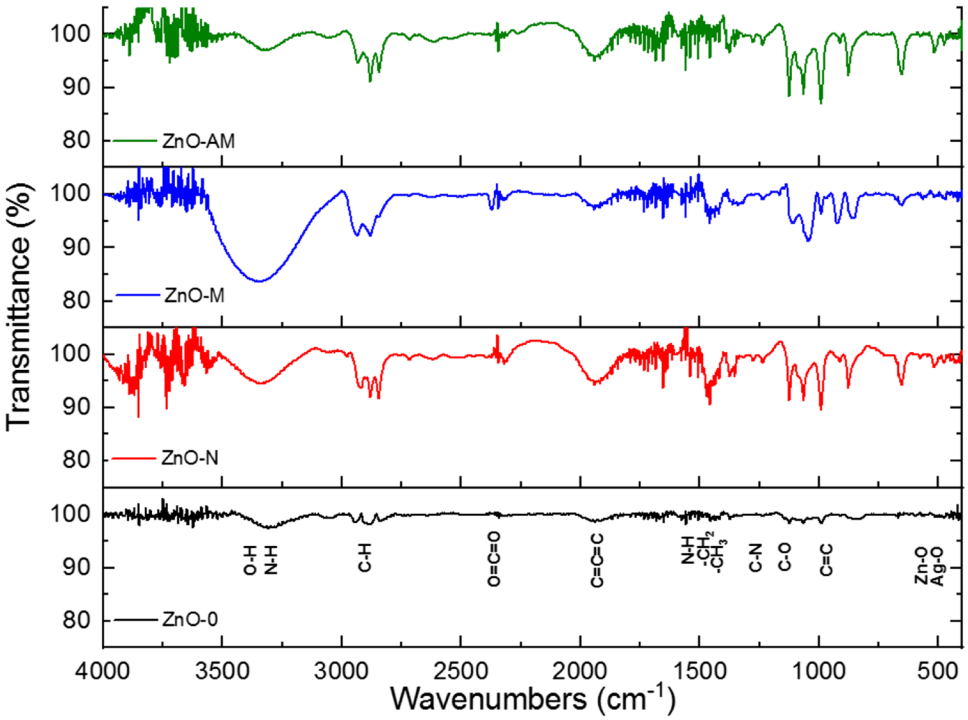

Fig. 3 FTIR spectra of the studied films

that these results are important to confirm the uniform distribution of additives throughout the films and they do not change/loose their physical or chemical characteristics. The uniform distribution can be attributed to high hydroxyl group content of PVA and glycerol that prevents the inorganic ZnO additives from agglomerating and results in homogeneous distribution of the particles in the chitosan/PVA matrix [43].

The characteristic functional groups were investigated through FTIR spectra of the studied films as shown in Fig. 3. A broad band at between 3200 and 3550 cm^{-1} represents the -OH stretching vibrations and the -NH bands of amine and amide. Absorption bands between 2840 and 3000 cm^{-1} can be attributed to the C-H symmetrical and unsymmetrical stretching vibration [44]. Absorption bands between 2320 and 2370 cm^{-1} are caused by atmospheric CO_2 [45] in the device and between 1900 and 2000 cm^{-1} correspond to C = C = C stresses. The peak at 1543 cm^{-1} belonging to the primary amine N–H bending vibration is clearly visible [46]. The -CH_2 bending and -CH_3 symmetrical stretching are clearly seen with the 1458 cm^{-1} and 1371 cm^{-1} bands, respectively. It is seen that the 1236 cm^{-1} band belongs to the C-N stretching vibration, and absorption bands between 1050 and 1155 cm^{-1} belong to the C-O stretching vibration [47]. Absorption bands between 875 and 995 cm^{-1} can be attributed to C = C symmetrical stretching vibration [48]. Absorption bands between 460 and 590 cm^{-1} represent the characteristic stretching mode of Zn–O and Ag–O bonds [45]. With the addition of inorganic ZnO powders to the films, characteristic bands shifted to lower wavelengths and their intensity increased. The reason for this is the formation of intermolecular hydrogen bonds between PVA, chitosan and ZnO. The peak at 1543 cm^{-1} (NH_2) belonging to the primary amine N–H bend are the characteristic peaks of chitosan. The reason that the intensity of the peak at 1543 cm^{-1} increases with the amount of ZnO is due to the increase in the intermolecular hydrogen bonds between –NH groups of chitosan and ZnO [49]. As shown in the figure, the highest intensity peaks are observed in the MicNo® system suggesting that the intermolecular bonding between the polymeric part and MicNo® particles was the highest in this system. Moreover, the FTIR spectra reveal the interaction between Ag and MicNo® platelets. Accordingly, this suggests that Ag must be in bonded form inside or on the surface of the MicNo® ZnO structure [50].

Figure 4 shows SEM micrographs of the films studied in this work. Although there are some regions of agglomerated ZnO particles, they are mostly homogeneously dispersed in the chitosan/PVA matrix. Agglomerate formation is higher in nano ZnO–containing films with respect to MicNo® ZnO containing films. These results also support what was deduced from the XRD patterns, as shown in Fig. 2b and c. It has been determined by SEM micrographs that MicNo® ZnO–containing film has high surface coverage and low agglomeration tendency. These results have already been supported by the average tensile strength and UV absorbance results. The high hydroxyl group content of PVA prevents inorganic ZnO additives from agglomerating and ensures homogeneous dispersion in the matrix [43].

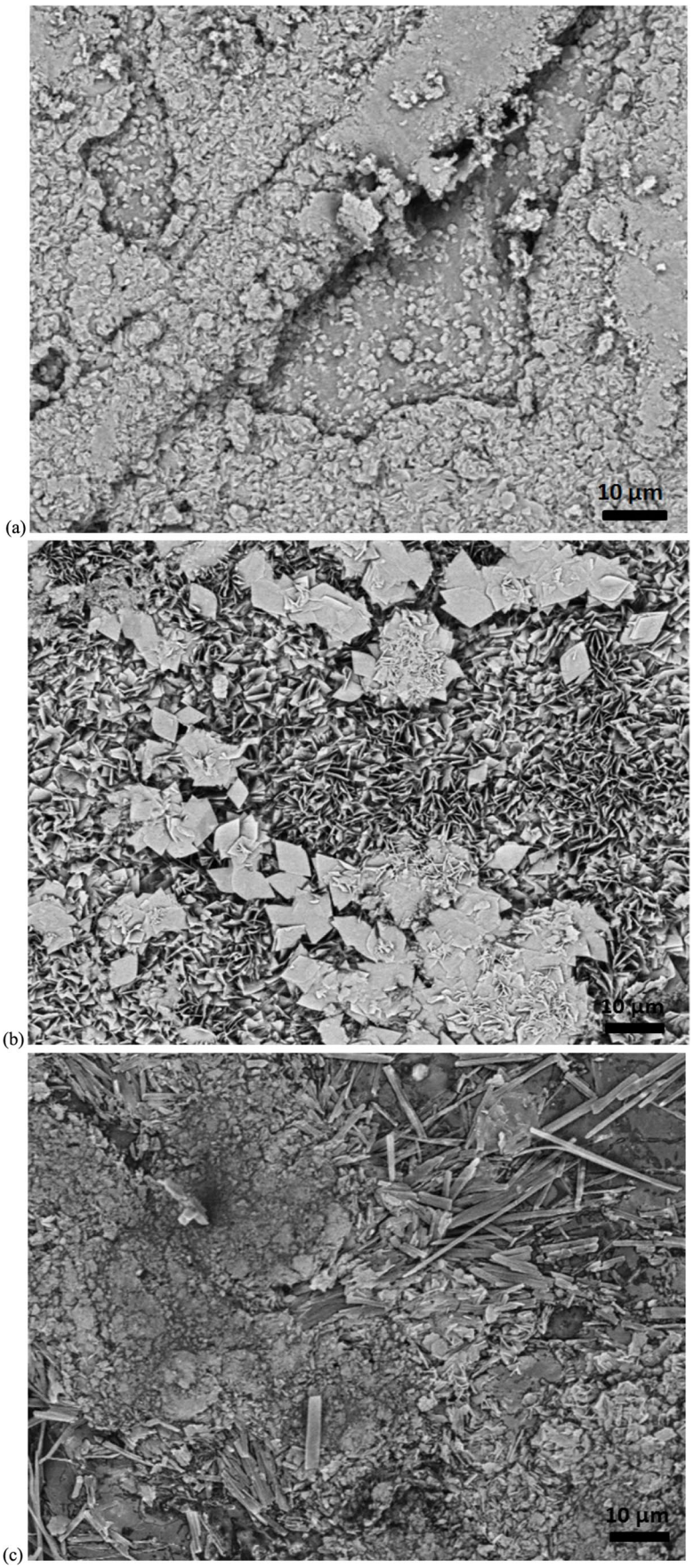

Fig. 4 SEM micrographs of the (**a**) ZnO-N, (**b**) ZnO-M, (**c**) ZnO-AM

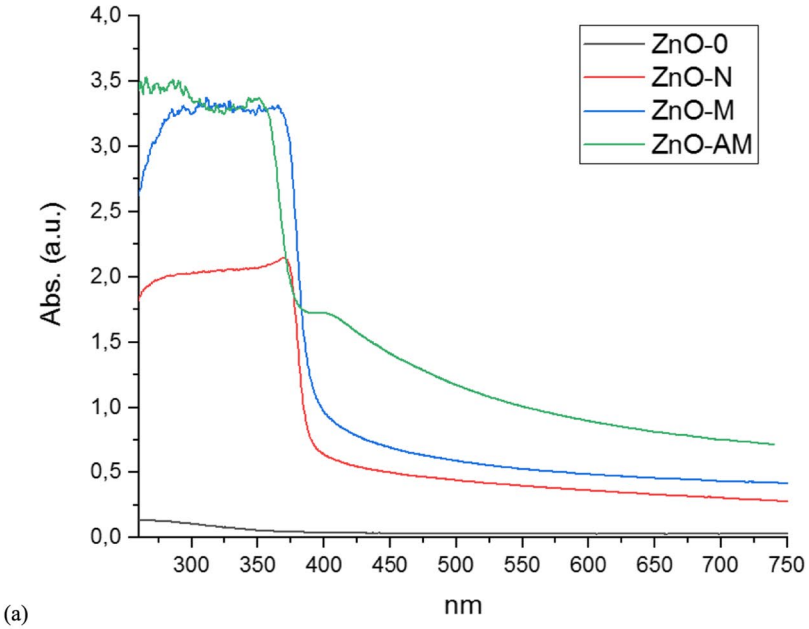

(a)

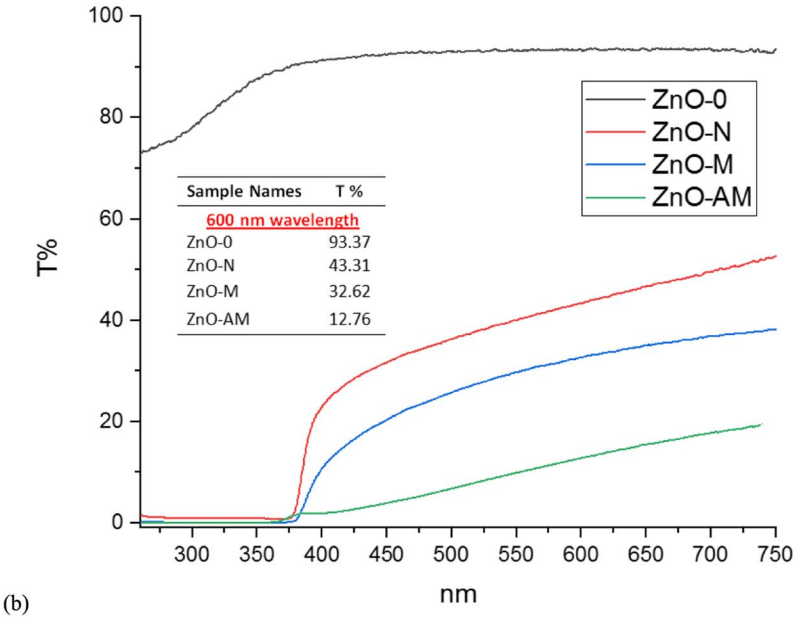

(b)

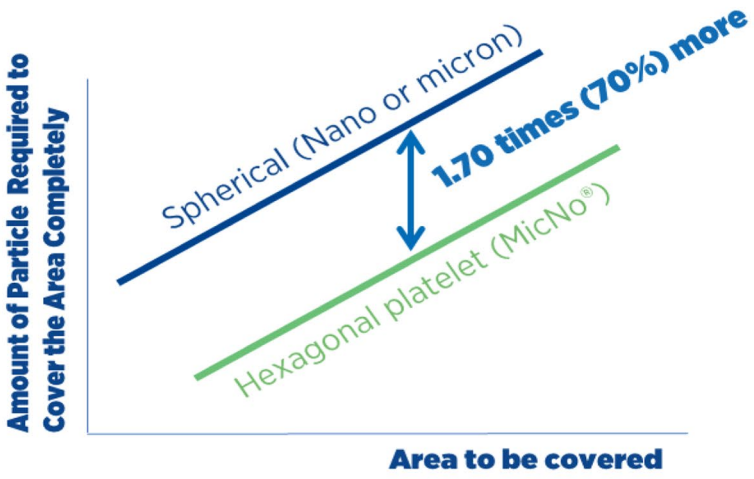

(c)

Fig. 5 (**a**) UV–vis absorbance, (**b**) UV–vis transparence spectra of the studied films (The transmittance values of the studied films at 600 nm wavelength inside the graph) and (**c**) MicNo® vs. spherical particles surface coverage ability comparison (**Assumptions:** MicNo.®: Hexagonal platelet (4 × 1.75 × 0.1 µm); nano: spherical (300 nm); no uncontrolled agglomeration)

Table 2 Average tensile strength (MPa) and % elongation values of the studied films

Sample name	Average tensile strength (MPa)	Average elongation (%)
ZnO-0	0.46	20.25
ZnO-N	0.73	15.52
ZnO-M	1.21	15.63
ZnO-AM	0.87	13.91

Table 3 The antibacterial activity (R) values against *S. aureus* and *E. coli* of the studied films

Sample name	*S. aureus* (R)	*E. coli* (R)
ZnO-0	0.10	0.38
ZnO-N	2.57	7.72
ZnO-M	6.91	7.76
ZnO-AM	7.72	7.80

Effects of MicNo® particles on optical, mechanical and antibacterial properties of the chitosan/PVA Films

Figure 5a, UV–Vis absorbance spectra of the films, prepared in this study, are given. It was observed that the amount of absorption increased in the UVA region (315–400 nm) when inorganic ZnO powders were added. The highest UV absorbance was demonstrated by MicNo® containing films. This can be attributed to higher surface covering ability of hexagonal ZnO particles than spherical nano particles. Figure 5c shows the difference between surface covering ability of hexagonal (e.g., MicNo®) and spherical particles. The surface covering ability property is a mathematical calculation. This calculation was made by using the amount of material required for the hexagonal and spherical shaped powders in the dimensions given in the graph to fully cover a certain surface area. While a single coat is required for hexagonal, several layers of powder are required for spherical to have full coverage. As shown in the figure, to cover the same area 70% more spherical particles are needed with respect to MicNo®. The increase in UV absorption intensity between 355 and 375 nm indicates that ZnO and chromophore groups are bonded in composite films [51]. In addition, when inorganic ZnO powder was added, the absorption bands shifted to higher wavelengths. This is probably due to the fact that, the hydrogen bonds formed between -OH groups in the PVA main chain and Zn^{+2} ions available on the ZnO powder surfaces [52]. The larger shift, in the MicNo® ZnO containing system than nano ZnO system also suggests the stronger molecular level interaction between the polymeric part and the MicNo® than nano particles. In UVA and UVB regions, higher absorption is expected in undoped MicNo® ZnO doping compared to Ag-doped MicNo® ZnO doping due to the higher surface area. However, an increase was observed in the absorption spectra in both UV and visible regions of Ag-doped MicNo® ZnO doped films. This may be attributed to both the interaction and transfer of electrons between Ag and ZnO and the "Surface Plasman Resonance (SPR)" absorption of silver particles [53]. These results suggest that the UV resistance of the films can be improved much more effectively by MicNo® particles with respect to nanoparticles. This outstanding performance enhancement can be attributed to much more effective surface covering ability of unique hexagonal morphology of MicNo® particles with respect to speherical nano particles. In addition, in Fig. 5b, UV–vis transmittance spectra of the studied films are shown. The transmittance values in the visible range (400–700 nm) are lower for Ag-doped than MicNo® ZnO–doped films, indicating that the transparency of this film is lower in the visible region. The transmittance values of the studied films at 600 nm wavelength are also presented in this figure.

Table 2 shows average tensile strength (MPa) and % elongation values of the studied films in this work. The average tensile strength value of ZnO-0 was 0.46 MPa and the average % elongation amount was 20.25%. An increase in tensile strength and a decrease in % elongation were observed with the addition of inorganic ZnO particles into the film. Whereas the tensile strength and the elongation values were 0.73 MPa and 15.52%, respectively, for the nano ZnO containing system, they were 1.21 MPa and 15.63%, respectively, for the MicNo® ZnO containing system. The reason for this change in mechanical strength is probably due to hydrogen bonds formed between PVA, chitosan and Zn^{+2} ions. In addition, this interaction restricts the movement of molecular chain segments, which causes a decrease in elongation [54]. As noted above, the average tensile strength and % elongation values of MicNo® ZnO added films were higher than nano ZnO added films. This can be attributed to stronger intermolecular interaction between MicNo® ZnO particles and the polymeric components than nano ZnO particles as confirmed by FTIR and UV–Vis results. It is known that during solution casting processes, the aggregation of ZnO particles dispersed in the polymer matrix reduces the physical cross-link strength between polymer blend chains and ZnO [55] and hence since probably nano particles exhibited higher aggregation, lower mechanical strength values were observed for nano particles with respect to MicNo®.

In Table 3, the antibacterial activity (R) values against *S. aureus* and *E. coli* of the studied films are shown. The

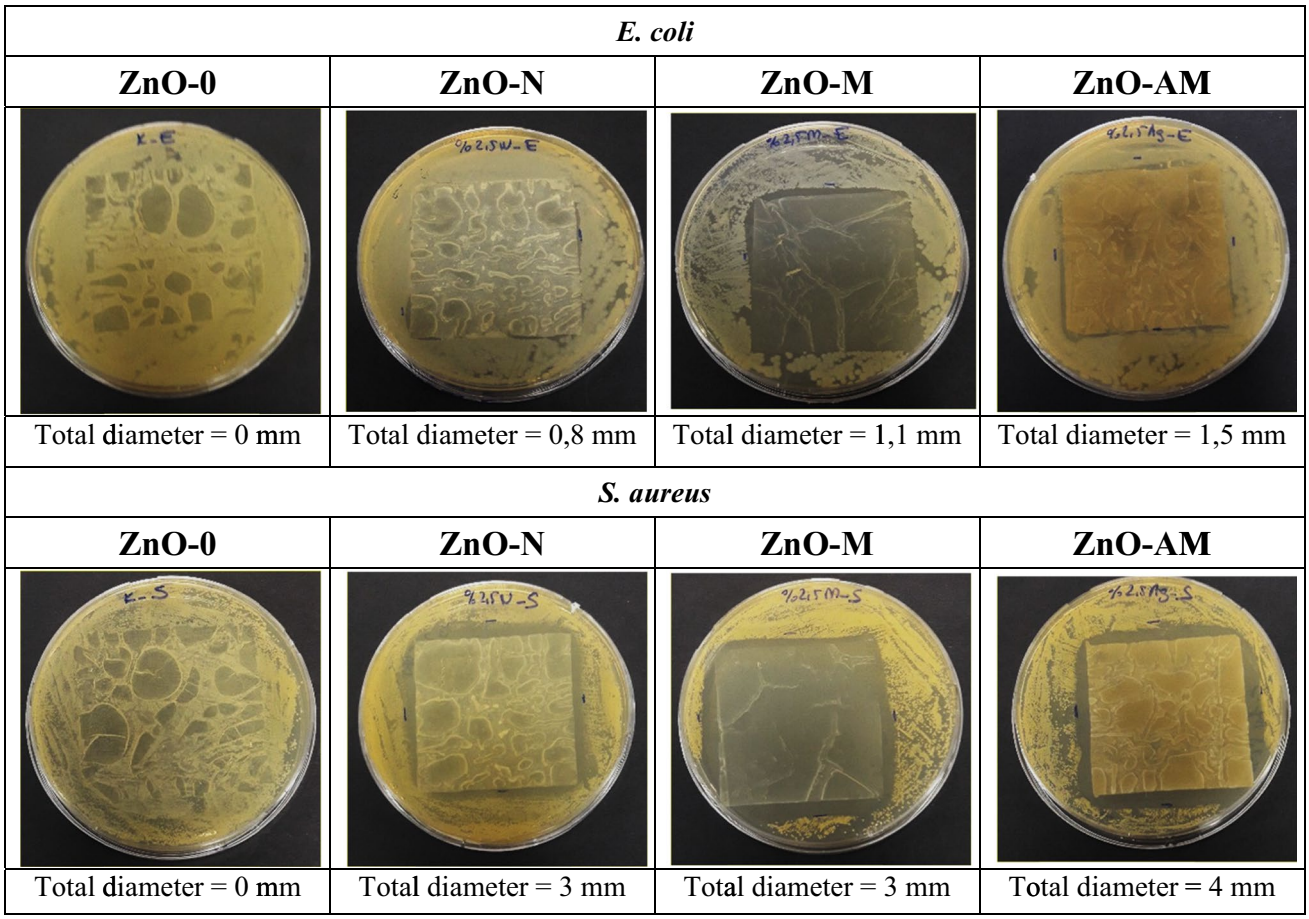

Fig. 6 Inhibition zone thicknesses (mm) against *E. coli* and *S. aureus*

antibacterial activity (R) values of studied films are higher against *E. coli*. These results are supported by the study of G. Nagaraju et al. [56]. ZnO-0 film does not exhibit adequate antibacterial effect. The R values of ZnO-0 film against *S. aureus* and *E. coli* are 0.10 and 0.38, respectively. With the addition of inorganic ZnO particles with high antibacterial activity into the films, the R values became compatible with the ISO 22196:2011 standard. There are mainly three propounded mechanisms for antibacterial activity of ZnO particles. There are (i) formation of reactive oxygen species, (ii) release of cytotoxic Zn^{2+} ions, (iii) the adsorption of ZnO particles onto the microbial cell walls [32, 57, 58]. As the specific surface area of ZnO increases, the contact surface area/volume between microorganisms and the particles increases as in the MicNo® case and this interaction makes the above mentioned third mechanism dominant [34]. Due to micron size and platelet shape of MicNo® ZnO powder, they cannot pass through the cytoplasm of the bacterial cell. Thus, cytotoxic and genotoxic behaviors are controlled by the concentration of Zn^{+2} ions dissolved from the particle surface. On the other hand, as we mentioned in Fig. 5c, the high surface coverage ability of MicNo® ZnO according to nano ZnO causes the cell to die earlier by preventing the passage of nutrients needed by the cell, to better cover the cell cytoplasm surface [36]. Therefore, the R values of the MicNo® ZnO–doped films were higher than the nano ZnO–doped films. The best results were seen with Ag-doped MicNo® ZnO-doped films. There are many mechanisms explaining the reasons for the increased antibacterial activity of Ag-doped ZnO powders. There are (i) the increase of perhydroxyl (H_2O_2) and strong oxidizing ($\cdot O_2^-$,$OH\cdot$) radicals reacting with bacteria as a result of the increase in the photocatalytic property of ZnO with silver doping [59], (ii) due to the fact that the ionic radius of Ag^+ ions (1.26 Å) is larger than the ionic radius of Zn^{+2} ions (0.74 Å), the substitutional of Ag^+ ions to the Zn^{+2} regions and this situation favors the easy release of Zn^{+2} ions from the lattice [60], (iii) increased adhesion of ZnO to the bacterial cell cytoplasm surface by the presence of strong electrostatic interaction between Zn^{+2}, Ag^+ and the negatively charged outer surface of the bacteria

[59], (iv) Ag^+ ions change the DNA synthesis by inhibiting the enzymatic system of the respiratory chain of the bacterial cell [61]. It is clear that in our study, the higher bacteriocidal effect [32] was seen against both gram negative and gram positive bacteria with MicNo® ZnO and Ag-doped MicNo® ZnO containing films. With the removal of the active substance from the environment, bacteria do not reproduce.

Inhibition zone assay is a qualitative method and antibacterial activity is only tested based inhibitory effects of the films. ISO 22196 standard is a quantitative method applied because it combines adsorption and inhibition of bacterial cells properties. Therefore, in this study, the antibacterial activities of the chitosan/PVA films were tested two different methods. The antibacterial effects depending on the solubility of the films were determined by the inhibition zone assay. Evaluation, zone formation is expected if there is active substance solubility from the sample, while no zone formation is expected if there is no solubility. The occurrence of the inhibition zone indicates that the tested ZnO powder systems have different levels of antibacterial activities on *E. coli* and *S. aureus* (Fig. 6) [34]. According to the results, it can be concluded that the films did not show antibacterial effect depending on solubility against to *E. coli*. However all inorganic powders appear to inhibit *S. aureus* (3–4 mm). Inhibition zone studies also confirm how non-antibacterial films are convex to antibacterial systems via addition of ZnO particles.

Conclusions

Chitosan/PVA/ZnO blend films were prepared via tape casting technique. MicNo® ZnO particles exhibited less agglomeration with respect to the nano ZnO particles which showed a better dispersion and surface coverage in chitosan/PVA matrix resulting to enhanced UV-resistance.

FTIR spectra reveal stronger chemical interaction between MicNo® ZnO and chitosan/PVA matrix than that of the nano ZnO and the matrix. This result is supported by higher tensile strength values. Addition of inorganic ZnO particles into the films resulted in increased tensile strength and decreased % elongation because of hydrogen bonds. Mechanical tests revealed the highest tensile strength in MicNo® ZnO added films because of stronger intermolecular interaction between the inorganic powder and polymeric component.

Chitosan/PVA films with inorganic ZnO additives exhibited reasonable transparency and demonstrated very high UV absorption capacities in UVA and UVB regions. Furthermore, both MicNo® ZnO and Ag-doped MicNo® ZnO containing films exhibited higher UV-absorbance values than nano ZnO particle containing films. These results suggest that the UV resistance of the films can be improved much more effectively by MicNo® particles with respect to nano particles. This outstanding performance enhancement can be attributed to much more effective surface covering ability of unique hexagonal morphology of MicNo® particles with respect to speherical nano particles.

Although the pristine film did not exhibit effective antibacterial activity, it has been shown that all ZnO-containing samples exhibited antibacterial activity at different levels. The antibacterial activity test showed that Ag-doped MicNo® ZnO embedded in chitosan/PVA matrix has the highest R values. At the same time, the antibacterial activity is higher for *E. coli* than for *S. aureus*.

These results clearly show that the tested chitosan/PVA/MicNo® ZnO composite films can be utilized as antibacterial polymeric materials with improved mechanical properties for biomedical applications such as wound healing as well as for novel applications in food industry as packaging material.

Acknowledgements The authors would like to thank Prof. Dr. Rasime Demirel for her contributions for the antibacterial tests. In addition, the fruitful discussions provided by Assoc. Prof. Dr. R. Bengü Karabacak, Prof. Drs. Murat Erdem and Mustafa Erdem Üreyen throughout this study are greatly acknowledged.

Funding This research was supported financially by the Eskişehir Technical University Scientific Research Projects Commission (Project number: 20DRP036).

Declarations

Conflict of interest The authors declare no competing interests.

References

1. HazarYoruç, A.B., Uğraşkan, V.: Yeşil Polimerler ve Uygulamaları. AKU J. Sci. Eng. **17**, 318–337 (2017). https://doi.org/10.5578/fmbd.53940
2. Wang, J., Zhuang, S.: Chitosan-based materials: preparation, modification and application. J. Clean. Prod. **355**, 131825 (2022). https://doi.org/10.1016/j.jclepro.2022.131825
3. Bano, I., Arshad, M., Yasin, T., Ghauri, M.A.: Preparation, characterization and evaluation of glycerol plasticized chitosan/PVA blends for burn wounds. Int. J. Biol. Macromol. **124**, 155–162 (2019). https://doi.org/10.1016/j.ijbiomac.2018.11.073
4. Yuvaraja, G., Pathak, J.L., Weijiang, Z., Yaping, Z., Jiao, X.: Antibacterial and wound healing properties of chitosan/poly(vinylalcohol)/zinc oxide beads (CS/PVA/ZnO). Int. J. Biol. Macromol. **103**, 234–241 (2017). https://doi.org/10.1016/j.ijbiomac.2017.05.020
5. Ravi Kumar, M.N.V.: A review of chitin and chitosan applications. React. Funct. Polym. **46**, 1–27 (2000). https://doi.org/10.1016/S1381-5148(00)00038-9
6. Guzmán, E., Ortega, F., Rubio, R.G.: Chitosan: A promising multifunctional cosmetic ingredient for skin and hair care. Cosmetics **9**, 99 (2022). https://doi.org/10.3390/cosmetics9050099
7. Al-Naamani, L., Dobretsov, S., Dutta, J.: Chitosan-zinc oxide nanoparticle composite coating for active food packaging

applications. Innov. Food Sci. Emerg. Technol. **38**, 231–237 (2016). https://doi.org/10.1016/j.ifset.2016.10.010
8. Hu, D., Wang, L.: Fabrication of antibacterial blend film from poly (vinylalcohol) and quaternized chitosan for packaging. Mater. Res. Bull. **78**, 46–52 (2016). https://doi.org/10.1016/j.materresbull.2016.02.025
9. Jridi, M., Hajji, S., Ayed, H.B., Lassoued, I., Mbarek, A., Kammoun, M., Souissi, N., Nasri, M.: Physical, structural, antioxidant and antimicrobial propertiesof gelatin-chitosan composite edible films. Int. J. Biol. Macromol. **67**, 373–379 (2014). https://doi.org/10.1016/j.ijbiomac.2014.03.054
10. Liu, Y., Wang, S., Zhang, R.: Composite poly(lactic acid)/chitosan nanofibrous scaffolds for cardiac tissue engineering. Int. J. Biol. Macromol. **103**, 1130–1137 (2017). https://doi.org/10.1016/j.ijbiomac.2017.05.101
11. Wang, H., Zhang, R., Zhang, H., Jiang, S., Liu, H., Sun, M., Jiang, S.: Kinetics and functional effectiveness of nisin loaded antimicrobial packaging film based on chitosan/poly (vinyl alcohol). Carbohydr. Polym. **127**, 64–71 (2015). https://doi.org/10.1016/j.carbpol.2015.03.058
12. Halima, N.B.: Poly(vinyl alcohol): review of its promising applications and insights into biodegradation. RSC Adv. **46**, 39823–39832 (2016). https://doi.org/10.1039/C6RA05742J
13. Yang, W., Owczarek, J.S., Fortunati, E., Kozanecki, M., Mazzaglia, A., Balestra, G.M., Kenny, J.M., Torre, L., Puglia, D.: Antioxidant and antibacterial lignin nanoparticles in polyvinyl alcohol/chitosan films for active packaging. Ind. Crops Prod. **94**, 800–811 (2016). https://doi.org/10.1016/j.indcrop.2016.09.061
14. Frone, A.N., Nicolae, C.A., Eremia, M.C., Tofan, V., Ghiurea, M., Chiulan, I., Radu, E., Damian, C.M., Panaitescu, D.M.: Low molecular weight and polymeric modifiers as toughening agents in poly(3-hydroxybutyrate) films. Polymers **12**, 2446 (2020). https://doi.org/10.3390/polym12112446
15. Fundo, J., Carvalho, A., Feio, G., Silva, Cristina L.M.., Quintas, M.: Relationship between molecular mobility, microstructure and functional properties in chitosan/glycerol films. Innov. Food Sci. Emerg. Technol. **28**, 81–85 (2015). https://doi.org/10.1016/j.ifset.2015.01.009
16. Ma, Y., Xin, L., Tan, H., Fan, M., Li, J., Jia, Y., Ling, Z., Chen, Y., Hu, X.: Chitosan membrane dressings toughened by glycerol to load antibacterial drugs for wound healing. Mater. Sci. Eng. C **81**, 522–531 (2017). https://doi.org/10.1016/j.msec.2017.08.052
17. Ghanbarzadeh B., Almasi H.: Biodegradable polymers, biodegradation-life of science. Chapter 6, in: Intech Open, R. Chamy (Eds) (2013). https://doi.org/10.5772/56230
18 Peponi, L., Puglia, D., Torre, L., Valentini, L., Kenny, José M.: Processing of nanostructured polymers and advanced polymeric based nanocomposites. Mater. Sci. Eng. R **85**, 1–46 (2014). https://doi.org/10.1016/j.mser.2014.08.002
19. Fan, M., Si, J., Xu, X., Chen, L., Chen, J., Yang, C., Zhu, J., Wu, L., Tian, J., Chen, X., Mou, X., Cai, X.: A versatile chitosan nanogel capable of generating AgNPs in-situ and long-acting slow-release of Ag^+ for highly efficient antibacteria. Carbohydr. Polym. **257**, 117636 (2021). https://doi.org/10.1016/j.carbpol.2021.117636
20. Akhtar, M.A., Ilyas, K., Dlouhý, I., Siska, F., Boccaccini, A.R.: Electrophoretic deposition of copper(II)–chitosan complexes for antibacterial coatings. Int. J. Mol. Sci. **21**, 263 (2020). https://doi.org/10.3390/ijms21072637
21. Brandelli, A., Ritter, A.C., Veras, F.F.: Antimicrobial activities of metal nanoparticles. In: Rai, Ph.D, M., Shegokar, Ph.D, R. (eds) metal nanoparticles in pharma. Springer, Cham. (2017). https://doi.org/10.1007/978-3-319-63790-7_15
22. Paszkiewicz, M., Gołąbiewska, A., Rajski, Ł., Kowal, E., Sajdak, A., Zaleska-Medynska, A.: Synthesis and characterization of monometallic (Ag, Cu) and bimetallic Ag-Cu particles for antibacterial and antifungal applications. J. Nanomater. **2016**, 11 (2016). https://doi.org/10.1155/2016/2187940
23. Tan, K.S., Cheong, K.Y.: Advances of Ag, Cu, and Ag-Cu alloy nanoparticles synthesized via chemical reduction route. J. Nanopart. Res. **15**, 1537 (2013). https://doi.org/10.1007/s11051-013-1537-1
24. Ali, H.M., Babar, H., Shah, T.R., Sajid, M.U., Qasim, M.A., Javed, S.: Preparation techniques of TiO_2 nanofluids and challenges: a review. Appl. Sci. **8**, 587 (2018). https://doi.org/10.3390/app8040587
25. Ghosh, M., Chakraborty, A., Mukherjee, A.: Cytotoxic, genotoxic and the hemolytic effect of titanium dioxide (TiO_2) nanoparticles on human erythrocyte and lymphocyte cells in vitro. J. Appl. Toxicol. **33**, 1097–1110 (2013). https://doi.org/10.1002/jat.2863
26 Kumar, S., Krishnakumar, B., Sobral, Abilio J.F.N.., Koh, J.: Bio-based (chitosan/PVA/ZnO) nanocomposites film: thermally stable and photoluminescence material for removal of organic dye. Carbohydr. Polym. **205**, 559–564 (2019). https://doi.org/10.1016/j.carbpol.2018.10.108
27 Jones, N., Ray, B., Ranjit, Koodali T., Manna, Adhar C.: Antibacterial activity of ZnO nanoparticles suspension on a broad spectrum of microorganisms. FEMS Microbiol. Lett. **279**, 71–76 (2008). https://doi.org/10.1111/j.1574-6968.2007.01012.x
28. Franklin, N.M., Rogers, N.J., Apte, S.C., Batley, G.E., Gadd, G.E., Casey, P.S.: Comparative toxicity of nanoparticulate ZnO, bulk ZnO, and $ZnCl_2$ to a freshwater microaga (Pseudokirchneriella subcapotata): the importance of particle solubility. Environ. Sci. Technol. **41**, 8484–8490 (2007). https://doi.org/10.1021/es071445r
29. Chauhan, R., Kumar, A., Tripathi, R., Kumar, A.: Advancing of zinc oxide nanoparticles for cosmetic applications. In: Handbook of consumer nanoproducts. Springer, Singapore. (2022). https://doi.org/10.1007/978-981-16-8698-6_100
30. Amornpitoksuk, P., Suwanboon, S., Sangkanu, S., Sukhoom, A., Muensit, N., Baltrusaitis, J.: Synthesis, characterization, photocatalytic and antibacterial activities of Ag-doped ZnO powders modified with a diblock copolymer. Powder Technol. **219**, 158–164 (2012). https://doi.org/10.1016/j.powtec.2011.12.032
31. Sharma, N., Kumar, J., Thakur, S., Sharma, S., Shrivastava, V.: Antibacterial study of silver doped zinc oxide nanoparticler against Staphylococcus aureus and Bacillus subtilis. Drug Invent. Today **5**, 50–54 (2013). https://doi.org/10.1016/j.dit.2013.03.007
32 Sirelkhatim, A., Mahmud, S., Seeni, A., Kaus, N.H.M., Ann, L.C., Bakhori, Siti K.M.., Hasan, H., Mohamad, D.: Review on zinc oxide nanoparticles: antibacterial activity and toxicity mechanism. Nano-Micro Lett. **7**(3), 219–242 (2015). https://doi.org/10.1007/s40820-015-0040-x
33 Hu, K., Kulkarni, Dhaval D., Choi, I., Tsukruk, Vladimir V.: Graphene-polymer nanocomposites for structural and functional applications. Prog. Polym. Sci. **39**, 1934–1972 (2014). https://doi.org/10.1016/j.progpolymsci.2014.03.001
34. Demirel, R., Suvacı, E., Şahin, İ, Dağ, S., Kılıç, V.: Antimicrobial activity of designed undoped and doped MicNo-ZnO particles. J. Drug Deliv. Sci. Technol. **47**, 309–321 (2018). https://doi.org/10.1016/j.jddst.2018.07.024
35. Sengun, P., Kesim, M.T., Caglar, M., Savaci, U., Turan, S., Sahin, İ, Suvaci, E.: Characterization of designed, transparent and conductive Al doped ZnO particles and their utilization in conductive polymer composites. Powder Technol. **374**, 214–222 (2020). https://doi.org/10.1016/j.powtec.2020.07.025
36. Genç, H., Barutca, B., Koparal, A.T., Özöğüt, U., Şahin, Y., Suvacı, E.: Biocompatibility of designed MicNo-ZnO particles: cytotoxicity, genotoxicity and phototoxicity in human skin keratinocyte cells. Toxicol. In Vitro **47**, 238–248 (2018). https://doi.org/10.1016/j.tiv.2017.12.004

37. Dermenci, K.B., Yanık, T., Dağ, S., Suvacı, E., Kesim, M.T., Savacı, U., Turan, S.: Electrochemical properties of ZnO anode materials with MicNo® morphology. Int. J. Ceram. Technol. **17**, 1882–1890 (2020). https://doi.org/10.1111/ijac.13486
38. Perelshtein, I., Ruderman, E., Perkas, N., Tzanov, T., Beddow, J., Joyce, E., Mason, Timothy J., Blanes, M., Mollá, K., Patlolla, A., Frenkel, Anatoly I., Gedanken, A.: Chitosan and chitosan–ZnO-based complex nanoparticles: formation, characterization, and antibacterial activity. J. Mater. Chem. B **14**, 1968–1976 (2013). https://doi.org/10.1039/C3TB00555K
39 Hezma, A.M., Rajeh, A., Mannaa, Mohammed A.: An insight into the effect of zinc oxide nanoparticles on the structural, thermal, mechanical properties and antimicrobial activity of Cs/PVA composite. Colloids Surf. A **581**, 123821 (2019). https://doi.org/10.1016/j.colsurfa.2019.123821
40. Yıldırım, Ö.A., Unalan, H.E., Durucan, C.: Highly efficient room temperature synthesis of silver-doped zinc oxide (ZnO:Ag) nanoparticles: structural, optical, and photocatalytic properties. J. Am. Ceram. Soc. **96**, 766–773 (2013). https://doi.org/10.1111/jace.12218
41. Ahn, B.D., Kang, H.S., Kim, J.H., Kim, G.H., Chang, H.W., Lee, S.Y.: Synthesis and analysis of Ag-doped ZnO. J. Appl. Phys. **100**, 093701 (2006). https://doi.org/10.1063/1.2364041
42. Yamada, M., Honma, I.: Anhydrous proton conductive membrane consisting of chitosan. Electrochim Acta **50**, 2837–2841 (2005). https://doi.org/10.1016/j.electacta.2004.11.031
43. Rashmi, S.H., Raizada, A., Madhu, G.M., Kittur, A.A., Suresh, R., Sudhina, H.K.: Influence of zinc oxide nanoparticles on structural and electrical properties of polyvinyl alcohol films. Plast. Rubber Compos. **44**, 33–39 (2015). https://doi.org/10.1179/1743289814Y.0000000115
44. Biazar, E., Zaeifi, D., Keshel, S.H., Ojani, S., Hajiaghaee, A., Safarpour, R., Sadeghpour, S.: Design of electrospun poly vinyl alcohol/chitosan scaffoldand its cellular study. AAB **6**(3), 46–51 (2015). https://doi.org/10.22037/jps.v6i3.9822
45. Waterhouse, G.I.N., Bowmaker, G.A., Metson, J.B.: The thermal decomposition of silver (I, III) oxide: a combined XRD, FT-IR and Raman spectroscopic study. Phys. Chem. **3**, 3838–3845 (2001). https://doi.org/10.1039/B103226G
46. Queiroz, F.M., Melo, K.R.T., Sabry, D.A., Sassaki, G.L., Rocha, H.A.O.: Does the use of chitosan contribute to oxalate kidney stone formation? Mar. Drugs **13**(1), 141–158 (2015). https://doi.org/10.3390/md13010141
47 Lim, S.-H., Hudson, Samuel M.: Synthesis and antimicrobial activity of a water-soluble chitosanderivative with a fiber-reactive group. Carbohydr. Res. **339**, 313–319 (2004). https://doi.org/10.1016/j.carres.2003.10.024
48. Vino, A.B., Ramasamy, P., Shanmugam, V., Shanmugam, A.: Extraction, characterization and in vitro antioxidative potential of chitosan and sulfated chitosan from Cuttlebone of Sepia aculeata Orbigny, 1848. Asian Pac. J. Trop. Biomed. **2**, 334–341 (2012). https://doi.org/10.1016/S2221-1691(12)60184-1
49 Vicentini, Denice S., Smania, A., Jr., Laranjeira, Mauro C.M..: Chitosan/poly (vinyl alcohol) films containing ZnO nanoparticles and plasticizers. Mater. Sci. Eng. C **30**, 503–508 (2010). https://doi.org/10.1016/j.msec.2009.01.026
50 Waterhouse, Geoffrey I.N.., Bowmaker, Graham A., Metson, James B.: The thermal decomposition of silver (I, III) oxide: a combined XRD, FT-IR and Raman spectroscopic study. Phys. Chem. Chem. Phys. **17**, 3838–3845 (2001). https://doi.org/10.1039/B103226G
51. Chouhan, S., Bhatt, R., Bajpai, A.K., Bajpai, J., Katare, R.D.: Investigation of UV absorption and antibacterial behavior of zinc oxide containing poly(vinyl alcohol-g-acrylonitrile) (PVA-g-PAN) nanocomposites films. Fibers Polym. **16**, 1243–1254 (2015). https://doi.org/10.1007/s12221-015-1243-y
52. Rithin Kumar, N.B., Crasta V., Praveen B.M.: Advancement in microstructural, optical, and mechanical properties of PVA (Mowiol 10–98) doped by ZnO nanoparticles. Phys. Res. Int. **2014**, 9 (2014). https://doi.org/10.1155/2014/742378
53. Saoud, K., Soubaihi, R.A., Saeed, S., Bensalah, N., Al-Fandi, M., Singh, T.: Heterogeneous Ag and ZnO based photocatalytic for waste water treatment under different irradiation conditions. J. Mater. Environ. Sci. **9**, 400–413 (2018). https://doi.org/10.26872/jmes.2018.9.2.44
54. Yin, M., Lin, X., Ren, T., Li, Z., Ren, X., Huang, T.-S.: Cytocompatible quaternized carboxymethyl chitosan/poly(vinyl alcohol) blend film loaded copper for antibacterial application. Int. J. Biol. Macromol. **120**, 992–998 (2018). https://doi.org/10.1016/j.ijbiomac.2018.08.105
55. Thiagamani, S.M.K., Rajini, N., Siengchin, S., VaradaRajulu, A., Hariram, N., Ayrilmis, N.: Influence of silver nanoparticles on the mechanical, thermal and antimicrobial properties of cellulose-based hybrid nanocomposites. Composites Part B **165**, 516–525 (2019). https://doi.org/10.1016/j.compositesb.2019.02.006
56. Nagaraju, G., Udayabhanu, Shivaraj, Prashanth, S.A., Shastri, M., Yathish, K.V., Anupama, C., Rangappa, D.: Electrochemical heavy metal detection, photocatalytic, photoluminescence, biodiesel production and antibacterial activities of Ag-ZnO nanomaterial. Mater. Res. Bull. **94**, 54–63 (2017). https://doi.org/10.1016/j.materresbull.2017.05.043
57. Pasquet, J., Chevalier, Y., Couval, E., Bouvier, D., Noizet, G., Morlière, C., Bolzinger, M.-A.: Antimicrobial activity of zinc oxide particles on five micro-organisms of the Challenge Tests related to their physicochemical properties. Int. J. Pharm. **460**, 92–100 (2014). https://doi.org/10.1016/j.ijpharm.2013.10.031
58. Pasquet, J., Chevalier, Y., Couval, E., Bouvier, D., Bolzinger, M.-A.: Zinc oxide as a new antimicrobial preservative of topical products: interactions with common formulation ingredients. Int. J. Pharm. **479**, 88–95 (2015). https://doi.org/10.1016/j.ijpharm.2014.12.031
59. Bechambi, O., Chalbi, M., Najjar, W., Sayadi, S.: Photocatalytic activity of ZnO doped with Ag on the degradation ofendocrine disrupting under UV irradiation and the investigation of its antibacterial activity. Appl. Surf. Sci. **347**, 414–420 (2015). https://doi.org/10.1016/j.apsusc.2015.03.049
60. Ravichandran, K., Sathish, P., Snega, S., Karthika, K., Rajkumar, P.V., Subha, K., Sakthivel, B.: Improving the antibacterial efficiency of ZnO nanopowders through simultaneous anionic (F) and cationic (Ag) doping. Powder Technol. **274**, 250–257 (2015). https://doi.org/10.1016/j.powtec.2014.12.053
61. Feng, Q.L., Wu, J., Chen, G.Q., Cui, F.Z., Kim, T.N., Kim, J.O.: A mechanistic study of the antibacterial effect of silver ions on Escherichia coli and Staphylococcus aureus. J. Biomed. Mater. Res. **52**, 662–668 (2000). https://doi.org/10.1002/1097-4636(20001215)52:4%3c662::AID-JBM10%3e3.0.CO;2-3